Anharmonicity of Coupled Torsions: The Extended Two-Dimensional Torsion Method and its Use to Assess More Approximate Methods

Luis Simón-Carballido,[†] Junwei Lucas Bao,[‡] Tiago Vinicius Alves,[¶] Rubén Meana-Pañeda,[§,‡] Donald G. Truhlar,[*,‡] and Antonio Fernández-Ramos[*,†]

[†]*Center for Research in Biological Chemistry and Molecular Materials (CIQUS) and Department of Physical Chemistry, University of Santiago de Compostela, 15782 Santiago de Compostela, Spain*

[‡]*Department of Chemistry, University of Minnesota, 207 Pleasant Street SE, Minneapolis, Minnesota 55455-0431, USA*

[¶]*Departamento de Físico-Química, Instituto de Química, Universidade Federal da Bahia, Rua Barão de Jeremoabo, 147, Salvador, Bahia, 40170-115, Brazil*

[§]*Laboratory of Computational Biology, NHLBI, National Institutes of Health, 5635 Fishers Lane, Suite T-906, Rockville, MD 20852, USA*

E-mail: truhlar@umn.edu; qf.ramos@usc.es

Abstract

In this work we present the extended two-dimensional torsion (E2DT) method and use it to analyze the performance of several methods that incorporate torsional anharmonicity more approximately for calculating rotational-vibrational partition functions. Twenty molecules having two hindered rotors were studied for temperatures between 100 and 2500 K. These molecules present several kinds of situation; they

include molecules with nearly separable rotors, molecules in which the reduced moments of inertia changes substantially with the internal rotation and molecules presenting compound rotation. Partition functions obtained by the rigid-rotor harmonic oscillator approximation, a method involving global separability of torsions and the multi-structural methods without explicit potential coupling [MS-T(U)] and with explicit potential coupling [MS-T(C)] of torsions are compared to those obtained with a quantized version -called the extended two-dimensional torsion (E2DT) method- of the extended hindered rotor approximation of Vansteenkiste et al. (J. Chem. Phys. **2006**, *124*, 044314). In the E2DT method, quantum effects due to the torsional modes were incorporated by the two-dimensional non-separable method, which is a method that is based on the solution of the torsional Schrödinger equation and that includes full coupling in both the kinetic and potential energy. By comparing other methods to the E2DT method and to experimental thermochemical data, this study concludes that: the harmonic approximation yields very poor results at high temperatures; the global separation of torsions from the rest of degrees of freedom is not justified even when an accurate method to treat the torsions is employed; it is confirmed that methods based on less complete potential energy coupling of torsions, such as MS-T(U), are not accurate when dealing with rotors with different barrier heights; and more complete inclusion of torsional coupling to the method in MS-T(C), improves substantially the results in such a way that it could be used in cases where the E2DT method is unaffordable.

1 Introduction

The calculation of rotational-vibrational (rovibrational) partition functions in flexible molecules is specially challenging if the goal is to evaluate accurate thermodynamic functions or thermal rate constants. Recent theoretical studies show that these objectives can be achieved by accounting for torsional anharmonicity[1] and multiple reaction paths.[2–6] The present work is concerned with the first of these two issues. An accurate calculation of rovibrational partition functions requires a good description of the coupling between the tops themselves and between the tops and the other degrees of freedom. However, it is quite common to calculate the rovibrational partition function within the rigid-rotor harmonic oscillator (RRHO) approximation, because it allows the separation of the rotational ($Q_{\rm rot}$) and vibrational ($Q_{\rm vib}^{\rm HO}$) partition functions, and it makes $Q_{\rm vib}^{\rm HO}$ be a product of easily calculated factors for individual normal modes that can be easily obtained from standard electronic structure programs, i.e.,

$$Q^{\rm RRHO} = Q_{\rm rot} Q_{\rm vib}^{\rm HO} \tag{1}$$

and

$$Q_{\rm vib}^{\rm HO} = \prod_{m=1}^{3N-6} \frac{e^{-\beta\hbar\omega_m/2}}{1-e^{-\beta\hbar\omega_m}} \tag{2}$$

where $\beta = k_{\rm B}T$, $k_{\rm B}$ is Boltzmann's constant, T is temperature; $\hbar$ is Planck's constant divided by 2π; $3N-6$ is the number of normal-mode vibrations of a non-linear polyatomic molecule (N is the number of atoms) and ω_m is the frequency of each of these vibrations.

In general, this approximation is better at low temperatures because under these conditions the partition function of a stable molecule is well described by a few levels belonging to the global minimum of the potential energy surface, and that of a transition state is well described by a few levels of the modes orthogonal to the reaction coordinate. However, as temperature rises the torsional motions, which usually involve low-frequency vibrational modes, are excited to high vibrational levels, and some molecules may have enough energy to overcome the torsional barriers and populate two or more minima of the potential energy

surface. Therefore, the methods that evaluate rovibrational partition functions in flexible molecules should include the anharmonic effect due to these torsions and incorporate it into the final result. Furthermore, torsions are often strongly coupled to overall rotation, and so one should include vibration-rotation coupling.

The works of Pitzer and Gwinn (PG)[7] and Kilpatrick and Pitzer (KP)[8] addressed the problem of how to calculate torsional partition functions even in situations involving strongly coupled torsions and torsions coupled with overall rotation. Much of the later research is based on finding approximations to and/or improvements to these two seminal works. However, there are aspects that were not discussed in depth in those two papers, but that are important to obtain accurate rovibrational partition functions, i.e., how to account more fully for anharmonicity in systems with multiple torsional minima, and how to incorporate the torsional partition function into the total rovibrational partition function. The original multi-structural method[9] MS-T(U) where U is shorthand for uncoupled torsional potential anharmonicity, and the multi-structural torsional anharmonicity method with effective barriers based on a coupled potential[10] [henceforth denoted MS-T(C) where C denotes coupled potential anharmonicity] try to answer these two questions. However, these two methods need further testing with a reference method allowing the analysis of their performance, and that is provided in the present article. We also compare the theoretical ideal gas-phase standard-state thermodynamic functions with the available experimental data.[11] These two issues are the goal of this work.

Recently, one of us developed the two-dimensional non-separable (2D-NS) method,[12] which can be used as a benchmark in the calculation of torsional partition functions in systems with two rotors. In the 2D-NS method the two-dimensional Schrödinger equation is solved by the variational method assuming that the two torsions are coupled in the kinetic and potential energy terms. This method[13] has been compared with other more approximate methods to treat torsions, such as the torsional eigenvalue summation[14] (similar to 2D-NS but using one-dimensional potentials) and the harmonic oscillator approximation. Here, for

the reference rovibrational partition function we use the extended hindered rotor (EHR) approximation of Vansteenkiste et al.,[15] which treats all the vibrational modes, except the torsions, as quantum harmonic oscillators. In the portion of the EHR treatment that we use here, the torsions are treated classically, but to be able to apply it at low temperatures, we include quantum effects using the 2D-NS method. We call this method the extended two-dimensional torsion (E2DT) method and use it as benchmark. (Note that Vansteenkiste et al.[15] also made a correction for quantum effects in the torsional modes, but at a less accurate level, and their correction is not tested here.)

For the comparison between methods we have chosen a series of 20 molecules, each of them with two hindered rotors. The molecules are depicted in Figure 1. The relative energies of the local torsional minima with respect to the global minimum are given in Table 1. There are molecules with nearly independent (nearly separable) rotors, for instance **S17**, molecules in which the two torsions are strongly coupled, such as **S7**, and molecules involving compound rotation (one rotating group is attached to the other rotating group), such as **S2**, **S8** and **S19**. There are also different types of rotors: symmetric tops (no off-balance term during rotation), in particular the methyl group, slightly asymmetric tops, in particular the -OH group, and very asymmetric tops, such as the -COH and the -CFH_2 groups. Therefore, the set is diverse, spanning from cases with nearly separable torsions with constant reduced moments of inertia to cases with coupled torsions with reduced moments of inertia that change substantially with internal rotation.

A brief description of the methods is given in section 2 and the comparison between them is discussed in section 4. The computational details are described in section 3, and section 5 summarizes the conclusions.

2 Methodology

The rotational-torsional classical partition function that includes full kinetic and potential energy couplings between torsions and between these torsions and the external rotation of a molecule with two torsions is given by[8]

$$Q_{\rm cl}^{\rm FC} = \frac{8\pi^2}{\sigma_{\rm tor}\sigma_{\rm rot}} \left(\frac{1}{2\pi\beta\hbar^2}\right)^{5/2} \int_0^{2\pi} \int_0^{2\pi} d\phi_1 d\phi_2 |\mathbf{S}(\phi_1,\phi_2)|^{1/2} {\rm e}^{-\beta {\rm V}(\phi_1,\phi_2)}, \tag{3}$$

where $Q_{\rm cl}^{\rm FC}$ means fully coupled (FC) classical partition function; $\sigma_{\rm rot}$ is the symmetry number for overall rotation;[16] $\sigma_{\rm tor} = \sigma_{\rm tor,1}\sigma_{\rm tor,2}$ is the product of the symmetry numbers for internal rotation $\sigma_{\rm tor,1}$ and $\sigma_{\rm tor,2}$ about the dihedral angles ϕ_1 and ϕ_2, respectively; $V(\phi_1,\phi_2)$ is the torsional potential; $|\mathbf{S}(\phi_1,\phi_2)|$ is the determinant of the rotational kinetic energy matrix, which after a congruent transformation (see ref 8) is given by:

$$|\mathbf{S}| = |\mathbf{D}| \prod_{i=1}^{3} I_i^{\rm rot} \tag{4}$$

where $I_i^{\rm rot}$ is one of the three principal moments of inertia and $|\mathbf{D}(\phi_1,\phi_2)|$ is the determinant of the $\mathbf{D}$ matrix. The $\mathbf{D}$ matrix accounts for the kinetic energy couplings between the two torsions and between the torsions and the external rotation:

$$\mathbf{D} = \begin{pmatrix} I_1 & -\Lambda_{12} \\ -\Lambda_{12} & I_2 \end{pmatrix} \tag{5}$$

The reduced moments of inertia of the two torsions are I_1 and I_2, and Λ_{12} is the coupling. The reduced moments of inertia can also be obtained by the method of Pitzer,[17] and they are commonly used in the evaluation of partition functions that consider torsions as separable ($\Lambda_{12} = 0$). Often, a good approximation is to assume that the principal moments of inertia do not change with the torsional angles, in which case we use the ones corresponding to the global minimum. With that assumption (which is made in some but not all of the methods

in this article), eq 3 is approximated to:

$$Q_{\rm cl}^{\rm FC} \cong Q_{\rm rot} Q_{\rm cl,tor}^{\rm (C)} \tag{6}$$

where

$$Q_{\rm rot} = \frac{8\pi^2}{\sigma_{\rm rot}} \left(\frac{1}{2\pi\hbar^2\beta} \right)^{3/2} \sqrt{I_1^{\rm rot} I_2^{\rm rot} I_3^{\rm rot}} \tag{7}$$

is the rotational partition function, and

$$Q_{\rm cl,tor}^{\rm (C)} = \frac{1}{\sigma_{\rm tor}} \frac{1}{2\pi\beta\hbar^2} \int_0^{2\pi} \int_0^{2\pi} d\phi_1 d\phi_2 |\mathbf{D}(\phi_1,\phi_2)|^{1/2} {\rm e}^{-\beta {\rm V}(\phi_1,\phi_2)}, \tag{8}$$

is the classical torsional partition function. In the case of symmetric tops eq 8 can be further simplified because $|\mathbf{D}(\phi_1,\phi_2)|$ is independent of the torsional angles, i.e.,

$$Q_{\rm cl,tor}^{\rm (C)\star} = \frac{1}{\sigma_{\rm tor}} \frac{1}{2\pi\beta\hbar^2} |\mathbf{D}|^{1/2} \int_0^{2\pi} \int_0^{2\pi} {\rm d}\phi_1 {\rm d}\phi_2 {\rm e}^{-\beta {\rm V}(\phi_1,\phi_2)} \tag{9}$$

It is convenient to fit the torsional potential to a Fourier series of the type:

$$\begin{aligned} V_{\rm tor}(\phi_1,\phi_2) =& V_1(\phi_1) + V_2(\phi_2) + \\ & \sum_{l_1=1}^{L_1} \sum_{l_2=1}^{L_2} c_{l_1 l_2} \cos(l_1\phi_1) \cos(l_2\phi_2) + \sum_{l_1'=1}^{L_1'} \sum_{l_2'=1}^{L_2'} c'_{l_1' l_2'} \sin(l_1'\phi_1) \sin(l_2'\phi_2) \end{aligned} \tag{10}$$

where $V_1(\phi_1)$ and $V_2(\phi_2)$ are one-dimensional potentials given by:

$$V_\tau(\phi_\tau) = a_{0,\tau} + \sum_{n_\tau=1}^{N_\tau} a_{n,\tau} \cos(n_\tau \phi_\tau)) \tag{11}$$

The parameters $c_{l_1 l_2}$ and $c'_{l_1' l_2'}$, as well as, the parameters for the one-dimensional potentials are obtained from the fitting. The potentials of eqs 10 and 11 may also include odd terms involving $\sin(n_1\phi_1)$, $\sin(n_2\phi_2)$, $\cos(l_1\phi_1)\sin(l_2\phi_2)$ or $\sin(l_1'\phi_1)\cos(l_2'\phi_2)$ functions, but they are seldom needed to obtain a good fit.

The torsional frequencies are calculated as the eigenvalues of the secular determinant:

$$|\mathbf{K} - \overline{\omega}_\eta^2 \mathbf{D}| = 0 \tag{12}$$

where

$$\mathbf{K} = \begin{pmatrix} \frac{\partial^2 V}{\partial \phi_1^2} & \frac{\partial^2 V}{\partial \phi_1 \partial \phi_2} \\ \frac{\partial^2 V}{\partial \phi_1 \partial \phi_2} & \frac{\partial^2 V}{\partial \phi_2^2} \end{pmatrix} \tag{13}$$

with the force constant matrix $\mathbf{K}$ of the torsional potential evaluated at the global minimum. These force constants can be obtained from the force constants associated to the torsions, which were calculated from the electronic structure calculations at the bottom of the potential or from the two-dimensional Fourier series potential used to fit the torsional potential. Except when otherwise indicated, the frequencies $\overline{\omega}_\eta$ are calculated from the Fourier series potential. Their values are listed in Table 1.

A quantum version of eq 8 for two coupled torsions is the 2D-NS method,[12,13] in which the torsional partition function is evaluated by directly solving the two-dimensional Schrödinger equation with full coupling in the kinetic, $T_{\rm tor}$, and potential energy terms, $V_{\rm tor}(\phi_1, \phi_2)$, i.e.:

$$\left\{ T_{\rm tor}\left(\frac{\partial}{\partial \phi_1}, \frac{\partial}{\partial \phi_2}\right) + V_{\rm tor}(\phi_1, \phi_2) \right\} \Phi(\phi_1, \phi_2) = E\Phi(\phi_1, \phi_2) \tag{14}$$

The kinetic energy is given by eq 8 of ref 12 and the potential is fitted to Fourier series. It includes the variation of the reduced moments of inertia with the torsions ϕ_1 and ϕ_2, as well as the coupling between these torsions. However, it does not include any term or coupling associated with the non-torsional degrees of freedom. Thus it does not include, for example, the Coriolis coupling between the internal rotors and the external rotors and the vibrational angular momentum of the $3N - 8$ vibrational modes. The Schrödinger equation of eq 14 is solved by the variational method. The trial function is built as a linear combination products of two one-dimensional wave functions that are solution of the Schrödinger equation for a

particle in a ring, i.e.,

$$\Phi(\phi_1, \phi_2) = \frac{1}{2\pi} \sum_{k_1=-K}^{K} \sum_{k_2=-K}^{K} c_{k_1,k_2} e^{ik_1\phi_1} e^{ik_2\phi_2} \tag{15}$$

where K is of the order of one hundred to obtain convergent results.

The 2D-NS partition function is obtained from the direct sum of the eigenvalues E_j obtained from eq 14 divided by the symmetry number due to the torsions, σ_{tor}:

$$Q_{\text{tor}}^{\text{2D-NS}} = \frac{1}{\sigma_{\text{tor}}} \sum_j e^{-\beta E_j} \tag{16}$$

and, therefore, the method can also be used to calculate the tunneling splitting of the lowest vibrational level due to torsional motion.[18]

The 2D-NS method is usually prohibitively expensive to extend to more than two degrees of freedom because of the size of the matrix to diagonalize when using the variational method. PG proposed an approximation that avoids to solve the Schrödinger equation, but corrects for quantum effects with a multiplicative factor F_{q} given by the ratio between the quantum and classical partition harmonic oscillator partition functions at the global minimum. The resulting torsional PG (TPG) partition function is given by:

$$Q_{\text{tor}}^{\text{TPG}} = \frac{Q_{\text{tor}}^{\text{HO}}}{Q_{\text{tor}}^{\text{CHO}}} Q_{\text{cl,tor}}^{(\text{C})} = F_{\text{q}}^{\text{TPG}} Q_{\text{cl,tor}}^{(\text{C})} \tag{17}$$

where

$$F_{\text{q}}^{\text{TPG}} = \frac{Q_{\text{tor}}^{\text{HO}}}{Q_{\text{tor}}^{\text{CHO}}} \tag{18}$$

The TPG partition function opens another possibility. It can be interpreted as an anharmonic correction to the harmonic oscillator torsional partition function (i.e., as the ratio between the fully coupled classical partition function and the classical limit of the harmonic

oscillator partition function). In this case

$$Q_{\rm tor}^{\rm TPG} = F_{\rm cl} Q_{\rm tor}^{\rm HO} \tag{19}$$

where

$$F_{\rm cl} = \frac{Q_{\rm cl,tor}^{\rm (C)}}{Q_{\rm tor}^{\rm CHO}} \tag{20}$$

There is no unique way to incorporate multiple torsional wells into the torsional partition functions of eqs 17 and 19. One possibility is to substitute the HO and CHO partition functions by multi-structural partition functions. The multi-structural HO and CHO partition functions are

$$Q_{\rm tor}^{\rm MS-HO} = \sum_{j=1}^{J} e^{-\beta U_j} \prod_{\eta=1}^{2} \frac{e^{-\beta\hbar\overline{\omega}_{j,\eta}/2}}{1-e^{-\beta\hbar\overline{\omega}_{j,\eta}}}, \tag{21}$$

and

$$Q_{\rm tor}^{\rm MS-CHO} = \sum_{j=1}^{J} e^{-\beta U_j} \prod_{\eta=1}^{2} \frac{1}{\beta\hbar\overline{\omega}_{j,\eta}}, \tag{22}$$

respectively. The torsional frequencies, $\overline{\omega}_{j,\eta}$ with $\eta = 1, 2$, are calculated for each well j through eq 12. The difference in energy between the global minimum and the well j is given by U_j of Table 1. An equation similar to eq 17 but taking into account multiple wells would be:

$$Q_{\rm tor}^{\rm MS-TPG} = F_{\rm q}^{\rm MS-TPG} Q_{\rm cl,tor}^{\rm (C)} \tag{23}$$

where

$$F_{\rm q}^{\rm MS-TPG} = \frac{Q_{\rm tor}^{\rm MS-HO}}{Q_{\rm tor}^{\rm MS-CHO}} \tag{24}$$

eq 23 can be considered to be an extension of the PG expression that takes into account multiple wells.

Torsional partition functions need to be integrated into the total rovibrational partition function to be used for calculating thermodynamic functions. One possibility is to start from the multi-structural rigid rotor harmonic oscillator (MS-HO) partition function, which

is given by

$$Q^{\mathrm{MS-HO}} = \sum_{j=1}^{J} Q_j^{\mathrm{RRHO}} \tag{25}$$

where Q_j^{RRHO} uses the same RRHO approximation as eq 1, but for each of the wells, i.e.,

$$Q_j^{\mathrm{RRHO}} = Q_{\mathrm{rot},j} Q_j^{\mathrm{HO}} e^{-\beta U_j} \tag{26}$$

where Q_j^{HO} is the product of individual mode partition functions in eq 1 evaluated for conformer j. The Boltzmann factor of eq 26 takes into account the difference in energy, U_j, between conformer j and the conformer corresponding to the global minimum. In a previous work, one of us introduced the following correction to the RRHO approximation:[12]

$$Q^{\mathrm{GS2DT}} = \alpha_{\mathrm{tor}}^{\mathrm{2D-NS}} Q^{\mathrm{MS-HO}} \tag{27}$$

where GS2DT means globally separable two-dimensional torsional method. The coefficient $\alpha_{\mathrm{tor}}^{\mathrm{2D-NS}}$ accounts for deviations from the MS-HO partition function:

$$\alpha_{\mathrm{tor}}^{\mathrm{2D-NS}} = \frac{Q_{\mathrm{tor}}^{\mathrm{2D-NS}}}{Q_{\mathrm{tor}}^{\mathrm{MS-HO}}} \tag{28}$$

The accuracy of this approximation is discussed in section 4.

Another possibility is to extend the torsional TPG partition function to all of the vibrational degrees of freedom. Instead of using the global separable approximation for torsions, the non-torsional degrees of freedom are incorporated into the classical partition function of eq 3.[15] This procedure accounts for the variation of the vibrational non-torsional degrees of freedom with the t torsions:

$$\begin{aligned} Q^{\mathrm{EHR}} =& \frac{8\pi^2}{\sigma_{\mathrm{tor}}\sigma_{\mathrm{rot}}} \left(\frac{1}{2\pi\beta\hbar^2}\right)^{3/2+t/2} \int_0^{2\pi}\int_0^{2\pi},\cdots,\int_0^{2\pi} d\phi_1 d\phi_2,\cdots,d\phi_{\mathrm{t}} \times \\ & |\mathbf{S}(\phi_1,\phi_2,\cdots\phi_{\mathrm{t}})|^{1/2} \mathrm{e}^{-\beta \mathrm{V}(\phi_1,\phi_2,\cdots,\phi_{\mathrm{t}})} \overline{\overline{\mathrm{Q}}}^{\mathrm{HO}}(\phi_1,\phi_2,\cdots,\phi_{\mathrm{t}}) \end{aligned} \tag{29}$$

The extended hindered rotor (EHR) partition function of eq 29 treats all the vibrational degrees of freedom, with the exception of the t torsions, quantum mechanically (within the harmonic approximation). The vibrational partition function $\overline{\overline{Q}}^{\rm HO}$ refers to the product of the individual vibrational harmonic $3N-6-t$ nontorsional vibrations and is given by:

$$\overline{\overline{Q}}^{\rm HO}(\phi_1,\phi_2,\cdots,\phi_{\rm t}) = \prod_{\overline{\overline{m}}=1}^{3N-6-t} \frac{e^{-\beta\hbar\overline{\overline{\omega}}_{\overline{\overline{m}}}(\phi_1,\phi_2,\cdots,\phi_{\rm t})/2}}{1-e^{-\beta\hbar\overline{\overline{\omega}}_{\overline{\overline{m}}}(\phi_1,\phi_2,\cdots,\phi_{\rm t})}} \tag{30}$$

where the non-torsional frequencies $\overline{\overline{\omega}}_{\overline{\overline{m}}}(\phi_1,\phi_2,\cdots,\phi_{\rm t})$ were calculated using nonredundant internal coordinates as detailed in ref 10.

In the case of two torsions ($t=2$) the EHR partition function is given by:

$$Q^{\rm EHR} = \frac{8\pi^2}{\sigma_{\rm tor}\sigma_{\rm rot}}\left(\frac{1}{2\pi\beta\hbar^2}\right)^{5/2}\int_0^{2\pi}\int_0^{2\pi} d\phi_1 d\phi_2 |\mathbf{S}(\phi_1,\phi_2)|^{1/2} {\rm e}^{-\beta {\rm V}(\phi_1,\phi_2)} \overline{\overline{\rm Q}}^{\rm HO}(\phi_1,\phi_2) \tag{31}$$

The interpolation of the $\overline{\overline{Q}}^{\rm HO}(\phi_1,\phi_2)$ partition function at different values of the two torsional angles is discussed in the Computational details section.

Quantum effects due to the torsions can be incorporated into the partition function of eq 31 as the ratio between quantum and classical torsional partition functions through a PG multiplicative coefficient similar to the one of eq 17, i.e.,

$$Q^{\rm EX} = F_{\rm q}^{\rm X} Q^{\rm EHR} \tag{32}$$

where X indicates the method used to calculate the two dimensional torsional partition function. It is also possible to use multi-structural partition functions as eq 24 or the 2D-NS partition function, that does not invoke the harmonic approximation. In this case the $F_{\rm q}^{\rm 2D-NS}$ is given by:

$$F_{\rm q}^{\rm 2D-NS} = \frac{Q_{\rm tor}^{\rm 2D-NS}}{Q_{\rm tor,cl}^{\rm (C)}} \tag{33}$$

and therefore our proposed extended two-dimensional torsion (E2DT) method is given by:

$$Q^{\mathrm{E2DT}} = F_{\mathrm{q}}^{\mathrm{2D-NS}} Q^{\mathrm{EHR}} \tag{34}$$

The E2DT method, in addition to the quantum effects due to the torsions, includes the variation of the external rotation and of the $3N$-8 vibrational degrees of freedom with the two torsions, as well as, the coupling between torsions. It can be considered an exact treatment of the two coupled torsions, also coupled as fully as possible to overall rotation and to nontorsional modes. Notice that the coupling between the two torsions and the overall rotation is treated classically through the $|\mathbf{S}|$ determinant. This coupling is not considered in the quantum correction of eq 33.

On the other hand, the TPG partition function of eq 19 shows that it is possible to correct the RRHO partition function for anharmonicity. If there are J distinguishable wells in the potential energy surface, the correction could be performed locally at every well. This is the basis of the multi-structural torsional (MS-T) methods. The rovibrational partition function is given by:

$$Q^{\mathrm{MS-T(Y)}} = \sum_{j=1}^{J} Q_j^{\mathrm{RRHO}} F_{\mathrm{cl},j}^{\mathrm{MS-T(Y)}} \tag{35}$$

where Y indicates one of the following two approaches: (i) the uncoupled potential Y=(U) multi-structural method with torsional anharmonicity [MS-T(U)] ; and (ii) coupled-potential Y=(C) multi-structural method with torsional anharmonicity [MS-T(C)]. The coefficients $F_{\mathrm{cl},j}^{\mathrm{MS-T(U)}}$ and $F_{\mathrm{cl},j}^{\mathrm{MS-T(C)}}$ are given by:

$$F_{\mathrm{cl},j}^{\mathrm{MS-T(U)}} = Z_j \prod_{\tau=1}^{t} f_{j,\tau} = Z_j \prod_{\tau=1}^{t} \frac{q_{j,\tau}^{\mathrm{RC(U)}}}{q_{j,\tau}^{\mathrm{CHO(U)}}} \tag{36}$$

in the uncoupled-potential version, and by:

$$F_{\mathrm{cl},j}^{\mathrm{MS-T(C)}} = \prod_{\eta=1}^{t} f_{j,\eta} = \prod_{\eta=1}^{t} \frac{q_{j,\eta}^{\mathrm{RC(C)}}}{q_{j,\eta}^{\mathrm{CHO(C)}}} \tag{37}$$

in the coupled-potential approximation. The $f_{j,\eta}$ factors evaluate the ratio between the classical anharmonic and classical harmonic oscillator torsional partition functions as in eq 20, but using approximations in the evaluation of the former. The definitions of Z_j, the classical $q_{j,\tau}^{\mathrm{RC(U)}}$ and $q_{j,\eta}^{\mathrm{RC(C)}}$, and the classical harmonic $q_{j,\tau}^{\mathrm{CHO(U)}}$ partition functions and $q_{j,\eta}^{\mathrm{CHO(C)}}$ are given below.

The main difference between the method of eq 35 and E2DT is that the latter is a global method, in the sense that it needs a knowledge of the whole torsional potential, whereas the MS-T(Y) methods are local and based on estimates of the anharmonicity in the surroundings of the wells. As a result the evaluation of the E2DT partition function is quite expensive in computer time (since the number of electronic structure calculations increases exponentially with the number of torsions), and therefore it is difficult to extend beyond two or three coupled torsions. In contrast the MS-T(Y) methods can readily be extended to higher dimensions.

The classical harmonic oscillator partition function in the MS-T(U) method is given by:

$$q_{\mathrm{j},\tau}^{\mathrm{CHO(U)}} = \frac{1}{\beta\hbar\overline{\omega}_{j,\tau}^{(\mathrm{U})}} \tag{38}$$

and the torsional frequencies of each well are calculated as:

$$\overline{\omega}_{j,\tau}^{(\mathrm{U})} = \sqrt{\frac{k_{j,\tau}}{I_{j,\tau}}} \tag{39}$$

where $I_{j,\tau}$ and $k_{j,\tau}$ are the reduced moment of inertia and the internal-coordinate force constant, respectively, for torsion τ in the well j. Assuming that the potential in the surroundings of minimum j is well represented by a reference PG potential, i.e., by a periodic potential with only one term in the cosine, for which we have the expression:

$$V_{j,\tau}(\phi_\tau) = U_j + \frac{1}{2}W_{j,\tau}^{(\mathrm{U})}[1-\cos M_{j,\tau}(\phi_\tau - \phi_{j,\tau,\mathrm{eq}})]; \quad \frac{-\pi}{M_{j,\tau}} \leq \phi_\tau - \phi_{j,\tau,\mathrm{eq}} \leq \frac{\pi}{M_{j,\tau}} \tag{40}$$

with $\phi_{j,\tau,\mathrm{eq}}$ being the torsional angle ϕ_τ at the equilibrium position. With this type of potential, the torsional frequency $\overline{\omega}_{j,\tau}^{(\mathrm{U})}$, the barrier height $W_{j,\tau}^{(\mathrm{U})}$ and the reduced moment of inertia $I_{j,\tau}$ are related by,

$$W_{j,\tau}^{(\mathrm{U})} = \frac{2I_{j,\tau}[\overline{\omega}_{j,\tau}^{(\mathrm{U})}]^2}{M_{j,\tau}^2} \tag{41}$$

With the potential of eq 40 the classical partition function can be integrated analytically yielding:

$$q_{j,\tau}^{\mathrm{RC(U)}} = \frac{\sigma_{\mathrm{tor},\tau}}{M_{j,\tau}} q_{\tau,j}^{\mathrm{FR}} \exp(-\beta W_{j,\tau}^{(\mathrm{U})}/2) I_0(\beta W_{j,\tau}^{(\mathrm{U})}/2) \tag{42}$$

where I_0 is a modified Bessel function of the first kind, $Q_{\tau,j}^{\mathrm{FR}}$ is the classical free-rotor partition function of torsion τ of well j and is given by

$$q_{\tau,j}^{\mathrm{FR}} = \frac{1}{\sigma_{\mathrm{tor},\tau}} \left(\frac{2\pi I_{\tau,j}}{\beta\hbar^2} \right)^{1/2} \tag{43}$$

It should be noticed that $\sigma_{\mathrm{tor},\tau}/M_{j,\tau}$ removes the torsional symmetry number of the free-rotor partition function and establishes the domain of well j through the local periodicity parameter $M_{j,\tau}$. This parameter is calculated through a Voronoi tessellation scheme.[1] Finally, the Z_j factor is given by

$$Z_j = g_j + (1 - g_j) Z_j^{\mathrm{int}} Z_j^{\mathrm{coup}} \tag{44}$$

The factor Z_j^{int} takes into account the coupling between torsions. It is given by the ratio between the coupled and uncoupled CHO partition functions:

$$Z_j^{\mathrm{int}} = \frac{\prod_{\eta=1}^{t} \overline{\omega}_{j,\eta}^{(\mathrm{C})}}{\prod_{\tau=1}^{t} \overline{\omega}_{j,\tau}^{(\mathrm{U})}} \tag{45}$$

where the product of the coupled torsional frequencies $\overline{\omega}_{j,\eta}^{(\mathrm{C})}$ is calculated as:

$$\prod_{\eta=1}^{t} \overline{\omega}_{j,\eta}^{(\mathrm{C})} = \frac{\prod_{m=1}^{F} \omega_{j,m}}{\prod_{\overline{\overline{m}}=1}^{F-t} \overline{\overline{\omega}}_{j,\overline{\overline{m}}}} \tag{46}$$

F being the number of vibrational degrees of freedom of the system; $\omega_{j,m}$ represents the normal mode frequencies at well j and $\overline{\overline{\omega}}_{j,\overline{\overline{m}}}$ are the nontorsional frequencies calculated in nonredundant internal coordinates.

On the other hand, the Z_j^{coup} term incorporates the coupling in the reduced moments of inertia through the ratio:

$$Z_j^{\text{coup}} = \left(\frac{|\mathbf{D}_j|}{\prod_{\tau=1}^{t} I_{j,\tau}} \right)^{1/2} \tag{47}$$

The factor g_j tends to the unity at low temperatures, where the rovibrational coupling is small and tends to zero at high temperatures. It is given by a switching function similar to the one used in ref 19:

$$g_j = \prod_{\tau=1}^{t} \tanh \left(\frac{\sigma_{\text{tor},\tau}}{M_{j,\tau}} \frac{q_{j,\tau}^{\text{FR}}}{q_{j,\tau}^{\text{CHO(U)}}} \right)^{1/t} \tag{48}$$

However, a given torsion may reach the high-temperature limit at a different rate than other torsions if the barriers they have to overcome are different. The coupled multi-structural method with torsional anharmonicity [MS-T(C)] solves this problem by removing the Z_j term and incorporating the couplings into the $f_{j,\eta}$ coefficients of eq 37. For the evaluation of the $q_j^{\text{CHO(C)}}$ partition function is enough to know the product of the coupled torsional frequencies $\overline{\omega}_{j,\eta}^{(\text{C})}$ of eq 46, whereas the evaluation of the reference coupled classical partition function about each well requires the calculation of coupled barrier heights, which are obtained from the eigenvalues $\tilde{\lambda}_{j,\eta}$ of the equation:

$$\tilde{\mathbf{F}}_j^{\text{tor}} = \mathbf{L}_j \mathbf{F}_j^{\text{tor}} \mathbf{L}_j \tag{49}$$

The force constant matrix $\mathbf{F}_j^{\text{tor}}$ in internal coordinates associated with the torsions includes the coupling between the torsions, and $\mathbf{L}_j$ is a diagonal matrix with elements given by $1/M_{j,\tau}$. The coupled torsional barriers are given by

$$W_{j,\eta}^{(\text{C})} = 2\tilde{\lambda}_{j,\eta}, \tag{50}$$

and the product of $q_{j,\tau}^{\mathrm{RC(C)}}$, which we call here $Q^{\mathrm{RC(C)}}$, is given by:

$$Q^{\mathrm{RC(C)}} = \prod_{\eta=1}^{t} q_{j,\eta}^{\mathrm{RC(C)}} = Z_j^{\mathrm{coup}} \prod_{\tau=1}^{t} \frac{\sigma_{\mathrm{tor},\tau}}{M_{j,\tau}} q_{\tau,j}^{\mathrm{FR}} \prod_{\eta=1}^{t} \exp(-\beta W_{j,\eta}^{(\mathrm{C})}/2) I_0(\beta W_{j,\eta}^{(\mathrm{C})}/2) \tag{51}$$

It should be noticed that neither $W_{j,\tau}^{(\mathrm{U})}$ nor $W_{j,\eta}^{(\mathrm{C})}$ correspond to calculated torsional barriers by electronic structure methods, but to effective torsional barriers. Thus, the multi-structural reference classical coupled torsional-rotational partition function [MS-RC(C)] given by

$$Q^{\mathrm{MS-RC(C)}} = \sum_{j=1}^{J} Q_{j,\mathrm{rot}} \prod_{\eta=1}^{t} q_{j,\eta}^{\mathrm{RC(C)}} \tag{52}$$

may be different from the classical fully coupled partition function of eq 3, although in the high-temperature limit both partition functions tend to the free rotor result, which is independent of the torsional barriers.

3 Computational details

All the electronic structure calculations were performed at the MPWB1K method,[20] with the minimally augmented polarized double-ζ basis set, 6-31+G(d,p).[21] This level of calculation performs well for nonmetallic thermochemical data and thermochemistry.[22] The energies, geometries and normal-mode frequencies of all the stationary points are listed in the Supporting Information. The 2D-NS method needs the construction of a global two-dimensional torsional potential energy surface for each molecule. Each point is obtained by partial optimization, i.e., all the internal coordinates of the molecule were optimized except the two torsions that were kept frozen. For the scan about the torsions we used a stepsize of 10°. The elements of the **D** matrix were calculated for each of the geometries as described in ref 8 and implemented in ref 9.

Notice that in this work all the calculated vibrational harmonic oscillator partition functions of all the systems, including those that used projected normal mode frequencies (after

removal of the torsional degrees of freedom), were scaled by the recommended scaling factor of 0.964.[23] Specifically, this scaling was applied to eqs 25 (through eq 26), 30, 35 and 46.

The two-dimensional torsional potential energy grid obtained from the electronic structure calculations was fitted to Fourier series, i.e. to a potential given by eq 10. The contour plots of those two-dimensional surfaces are displayed in Figures 2 and 3. All classical partition functions that needed integration were evaluated by the trapezoidal rule with a stepsize of 1°. The **D** matrix was also fitted to Fourier series having the same terms as the potential. All this information is listed in the Supporting Information. The fits to Fourier series were carried out by the *GNUplot* program.[24]

The evaluation of the $\overline{\overline{Q}}^{\mathrm{HO}}(\phi_1, \phi_2)$ partition function at specified values of the two torsional angles, which is needed in the calculation of the EHR partition function, involved the following steps: (i) evaluation of the force constants matrix (Hessian) at the stationary points (minima, transition states and maxima); (ii) removal of the torsional frequencies; (iii) interpolation of $\overline{\overline{Q}}^{\mathrm{HO}}$ at non-stationary structures.

Step (i) is straightforward because the search is directly carried out on the fitted Fourier series potential; once the stationary points are located the Hessian can be evaluated by standard quantum chemistry programs.

Step (ii) involves the separation of torsions from the other degrees of freedom. This is achieved by a transformation of the Hessian in Cartesian coordinates into a Hessian in internal coordinates, in which the torsions are explicitly defined without redundancies and removed from the the rest of the $3N$-8 degrees of freedom by using the procedure described in ref 10. This allows the calculation of $\overline{\overline{\omega}}_{\overline{\overline{m}}}$ and, therefore, of $\overline{\overline{Q}}^{\mathrm{HO}}$ at the stationary points.

For Step (iii), first we divide each of the two-dimensional surfaces into Delaunay triangles using the software package TRIPACK of Renka.[25] The vertices of the triangles correspond to stationary points, so at these locations the rovibrational partition function is available. If the value of the partition function is needed in an edge or inside the triangle, we need to obtain it by interpolation. Specifically, we have used modified hyperbolic tangent functions

to interpolate the edges in such a way that at each vertex the partition function coincides with the calculated value and at each edge the hyperbolic tangent reaches half its value when the difference between the potentials of the vertices is also half. For a point inside a triangle the partition function is obtained by building three additional triangles in which two of the points are the vertices and the third point is the one at which the partition function has to be obtained. By calculating the three heights of the triangles and taking as bases the edges, the interpolated partition function is given by the projected value over the edge with the shortest height. This procedure is difficult to extend to higher dimensions, so we have also tried a simpler approximation consisting in approximating the partition function at non-stationary points by the one at the stationary point with the shortest distance between them. The partition functions obtained by both approximations are practically identical at high temperatures and about 1% different at the lowest temperatures. For a given point at the edge or inside the triangle we approximate the partition function by the one at the vertex with the shortest distance between the point an the vertex.

The eigenvalues needed to obtain the 2D-NS partition functions were calculated with the *JADAMILU* software.[26] The torsional 2D-NS partition function and the GS2DT and E2DT rovibrational partition functions were obtained by the *HR2D* program.[27] The MS-T(U) and MS-T(C) partition functions were calculated with the *MSTor* program.[9,28] For each molecule all the electronic structure geometries and frequencies of the conformations are listed in the Supporting Information. All the electronic structure calculations were performed using the *Gaussian 09* program.[29]

4 Results and discussion

In the temperature range from 100 and 2500 K, we compare the MS-HO, MS-T(U), MS-T(C) and GS2DT rovibrational partition functions with the ones obtained by the E2DT method. Deviations of the data P from the benchmark results P_{ref} for the set of $N_{\mathrm{s}} = 20$

molecules $\mathbf{S}\ell$ ($\ell = 1, 2, \ldots, 20$) at temperature T are given by the mean unsigned percentage error (MUPE):

$$\text{MUPE-P-X}(T) = \frac{100}{N_\text{s}} \sum_{\ell=1}^{N_\text{s}} \left| \frac{P_\text{ref}^\text{X}(\ell, T) - P^\text{X}(\ell, T)}{P_\text{ref}^\text{X}(\ell, T)} \right| \tag{53}$$

where X indicates the method by which the data have been obtained. The data to be compared are partition functions [Q or $\tilde{Q}$ calculated from the bottom of the potential or from the zero-point energy (ZPE) of the global minimum, respectively], ratios between partition functions (PG factors) or thermodynamic functions. The benchmark data for the partition functions were obtained by the E2DT method, whereas in the case of the thermodynamic functions they were obtained from the literature.[11] In the case of the ideal gas-phase standard-state (pressure of 1 bar) thermodynamic functions, the data used to calculate the MUPEs were calculated as $P = \exp[-\Delta_0^T G^\circ/RT]$ and $P = \exp[-\Delta_0^T H^\circ/RT]$, in the case of the free energy and enthalpy, respectively; R is the ideal gases constant. The values $\Delta_0^T G^\circ$ and $\Delta_0^T H^\circ$ correspond to the free energy G° and enthalpy H°, respectively, referred to the enthalpy at $T = 0$ K. In the case of the entropy, S°, the data were calculated as $P = \exp(S^\circ/R)$.

Before discussing the results for the rovibrational partition functions, it is interesting to compare the multi-structural reference classical rotational-torsional partition function $Q^{\text{MS}-\text{RC(C)}}$ of eq 52 with the full classical partition function of eq 3 (taken as the benchmark). The MUPE decreases as temperature increases. For instance at $T = 300$ K the MUPE is 14%, at $T = 1000$ K is 11% and at $T = 1000$ K is 8%. The largest percentage errors (PEs) at both low and high temperatures correspond to system **S6** with values of 43% and 27% at 100 and 2500 K, respectively. The advantage of the classical partition function $Q^{\text{MS}-\text{RC(C)}}$ over $Q^{\text{FC(C)}}$ is that the former only needs information about the minima. Therefore, for most of the systems $Q^{\text{MS}-\text{RC(C)}}$ performs well at high temperatures, but is less accurate at low temperatures, because the importance of the shape of the potential is more important at those temperatures.

The zero-point energy of the E2DT partition function is given by the contribution of

the 3N-8 nontorsional degrees of freedom plus the lowest energy level obtained by direct diagonalization of the 2D-NS torsional partition function. For molecules as **S1**, **S2** or **S6** this ZPE is substantially different from the one obtained by normal-mode analysis (see Table 2). In general, the normal mode frequencies associated with the torsions are lower when coupled torsional frequencies are being considered (Table 1), so at very low temperatures the E2DT partition function may be larger (higher density of states) than the harmonic oscillator one. As temperature rises this effect reverses quite rapidly (the E2DT partition function becomes lower than the MS-HO partition function) if there are other minima available, and the barriers between them are not too high, so those minima can be reached. This is for instance the case of molecule **S2** that has a barrier between the two degenerate minima of only 116 cm^{-1}. On the other hand, **S1** and **S6** have large barrier heights between the minima with the lowest energy and each well behaves close to a harmonic oscillator, but with torsional frequencies with lower frequencies than the normal mode frequencies associated to the torsions. The effect of having different ZPE thresholds shows in the MUPEs at low temperatures. Thus, MUPE-Q at $T = 150$ K is 19% for the MS-HO and the MS-T(U) methods and 21% for the MS-T(C) method. At $T = 300$ K MUPE-Q increases to 21% and 24% for the MS-HO and MS-T(U) methods, respectively, but it decreases to 15% for the MS-T(C) method.

Pitzer[8] and KP suggested that it might be better not to add the geometry dependence of the moments of inertia unless one also accounts for the geometry dependence of the vibrational treatment (for example, one could use instantaneous normal modes to account for vibrational contributions away from stationary points). Therefore it is interesting to know the effect of such variation on the EHR partition function by comparing these results with the EHR partition function with constant ZPE and **D** values obtained at the global minimum geometry.

This one-well EHR partition function (1W-EHR) is given by:

$$Q^{\mathrm{1W-EHR}} = \frac{8\pi^2}{\sigma_{\mathrm{tor}}\sigma_{\mathrm{rot}}}\left(\frac{1}{2\pi\beta\hbar^2}\right)^{5/2} Q_{\mathrm{rot}}\overline{\overline{Q}}^{\mathrm{HO}}|\mathbf{D}|^{1/2}\int_0^{2\pi}\int_0^{2\pi}\mathrm{d}\phi_1\mathrm{d}\phi_2\mathrm{e}^{-\beta\mathrm{V}(\phi_1,\phi_2)} \qquad (54)$$

As expected, at low temperatures both results are quite similar, except for molecules **S7** and **S9** with percentage errors of 18% and 20% at $T = 150$ K. The reason is that these two molecules present very low energy minima with values of 50 (**M2-S7**) and 3 cm^{-1} (**M2-S9**) with respect to their global minimum **M1-S7** and **M1-S9**, respectively. The ZPE increases this difference in the case of **M2-S7** by 35 cm^{-1} and in the case of **M2-S7** by 27 cm^{-1}, therefore, the 1W-EHR partition function is larger than the normal EHR partition function of eq 31. For the rest of molecules the percentage errors are smaller or even negligible, and at $T = 150$ K the MUPE is only 4%. At $T = 300$ K the MUPE is still 4% but at higher temperatures starts to increase and at $T = 1000$ K is 10% and at $T = 2500$ K is 18%. As temperature increases the MUPE also increases because the normal EHR partition function starts to have important contributions from the transition states and maxima. In general, these stationary points have lower ZPEs than the minima resulting in a reduction of the classical potential and therefore in the increase of the normal EHR partition function with respect to the 1W-EHR partition function. Therefore, the approximation is not justified at high temperatures, and at low temperatures its applicability is limited to systems with an important difference in energy between the global minimum and the local minima.

On average quantum effects decrease the classical partition function (with zero of energy at the bottom of the well) by about 80% at $T = 150$ K, but only by 15% at $T = 300$ K. These quantum effects were incorporated into the EHR partition function as the ratio between the quantum 2D-NS and the torsional classical partition function. However, if the 2D-NS partition function is not available, quantum effects can be incorporated through any of the methods discussed in section 2. At $T = 150$ K the MUPEs associated with the PG factors given by the TPG and MS-TPG methods with respect to $F^{\mathrm{2D-NS}}$ are 6 and 5%, respectively.

The small difference between the TPG and MS-TPG methods shows that quantum effects can successfully be reproduced by the ratio between the quantum and classical harmonic oscillator at the global minimum. The MUPEs decrease to less than 3% at $T = 300$ K. Notice that this approximation is the same as the one assuming that the deviations from the harmonic oscillator given by the quotient $Q^{\mathrm{2D-NS}}/Q^{\mathrm{MS-HO}}_{\mathrm{tor}}$ in the quantum formulation are very similar to those given by the quotient using the classical expression, $Q^{(C)}_{\mathrm{cl,tor}}/Q^{\mathrm{MS-CHO}}_{\mathrm{tor}}$. Thus, the ratio

$$R = \frac{Q^{\mathrm{2D-NS}}_{\mathrm{tor}}/Q^{\mathrm{MS-HO}}_{\mathrm{tor}}}{Q^{(\mathrm{C})}_{\mathrm{cl,tor}}/Q^{\mathrm{MS-CHO}}_{\mathrm{tor}}} \tag{55}$$

should be very close to unity. Therefore this approximation, which has been incorporated into the multi-structural method to avoid the evaluation of torsional quantum partition function, is justified. However, it is important to use torsional frequencies instead of normal-mode frequencies in the evaluation of the PG coefficients accompanying the EHR partition function. At $T = 150$ K the MUPE doubles its value when normal-mode frequencies are used instead of torsional frequencies.

The effect of including a global correction to the torsional anharmonicity can be checked by comparing the GS2DT partition function of eq 27 with that obtained by the E2DT method. At $T = 150$ K the PEs are quite large for systems **S1**, **S6** and **S20** with values of 33%, 70% and 47%, respectively, and the MUPE is 14%. As temperature increases the MUPE remains constant but increases slightly at very high temperatures reaching 17% at $T = 2500$ K (see Figure 4). These results indicate that to incorporate torsional anharmonicity on top of the MS-HO partition function, even when full couplings in the kinetic and potential energies are taken into account, may lead to substantial errors. Some of us have used eq 27 to study the the hydrogen abstraction from ethanol by atomic hydrogen,[30] but for the ethanol molecule the MUPEs between the E2DT and the GS2DT partition functions were always between 6 and 8% in the whole range of temperatures studied in this work.

Hereafter, to establish a more direct comparison of the E2DT method with other methods that evaluate the rovibrational partition function, but have different thresholds for the ZPEs,

we compare rovibrational partition functions that are referred to the ZPE of the global minimum, instead of to the bottom of the potential. In such comparison anharmonic effects due to the ZPE are diminished. The comparison of MUPE-Q and MUPE-$\tilde{Q}$ is given in Figs 4 and 5, which show that there is an increase of the former with respect to the latter by about 10% at $T = 150$ K. This difference is reduced to only 3% at $T = 300$ K. Moreover, ZPE-exclusive partition functions can also be used in the comparison between theoretical and experimental thermodynamic functions, i.e., the entropy and the constant-pressure heat capacity are independent of the ZPE of the system and the free energy and the enthalpy are always referred to a reference state, which in general is the value of the enthalpy at $T = 0$ K, so the effect of the ZPE is also removed in this case.

Figure 4 shows that at $T \leq 200$ K the harmonic oscillator and the MS-T(U) approximations, which involve uncoupled torsions to the partition functions, agree quite well with those obtained by the E2DT method. Notice that at low temperatures the MS-HO partition functions are as good as the ones of anharmonic methods, but at room temperature the MUPE is already 16%. As temperature increases the harmonic oscillator partition function deviates substantially from the benchmark results, the MUPE being 82% at $T = 2500$ K. In general the harmonic approximation leads to partition functions which are too high (with the exception of molecules **S1** and **S6** discussed above). The reason is that at high temperatures the space available to the molecular system is too large in the harmonic oscillator model, because the harmonic oscillator is defined in the space $-\infty \leq \phi \leq +\infty$, whereas the internal rotation is restricted to $-\pi \leq \phi \leq +\pi$. At low temperature, the population of the harmonic oscillator outside of $-\pi \leq \phi \leq +\pi$ is negligible, but at high temperature, it dominates the error. Surprisingly the MS-HO partition functions yield values with smaller MUPEs than the ones obtained by the MS-T(U) method at temperatures $T \leq 500$ K. The best results are obtained with the MS-T(C) method, which improves substantially the MS-T(U) method above $T = 200$ K. The largest MUPE for the MS-T(C) is 14% and occurs at $T = 2500$ K.

In general, methyl groups are weakly coupled to other torsions, and the torsional potential

has a periodicity of 120°. One would expect a better performance of the anharmonic methods with respect to the benchmark results when the MUPE only includes this type of tops. This is the case for the MS-T(C) for which the MUPE drops to 7% at $T = 2500$ K. However, the MS-T(U) method performs worse for molecules having methyl groups than for the whole set. Specifically, the MUPE reaches its highest value of 41% at $T = 500$ K [the MUPE for the MS-T(C) at this temperature is 9%]. At $T = 500$ K the largest percentage error is for system **S15** with a value of 169%; the two rotating tops of this molecule are the -CH_3 and the -COH groups, with torsional barriers with regards to the global minimum of 419 and 2508 cm^{-1}, respectively. The two barriers for internal rotation are very different, so both tops reach the high temperature limit at very different thresholds. This situation cannot be handled properly by the switching function of eq 48, but it is properly taken into account by the MS-T(C) method for which the percentage error decreases to 1%.

Values for thermodynamic functions and based at least in part on experimental data are available from the literature[11] for systems **S4**, **S16** and **S17** for temperatures from 100 to 2500 K and for **S5** and **S20** in the interval from 100 to 1500 K. In fact the data extracted from ref 11 are taken from experiments or from an average of experimental data at temperatures near room temperature. Therefore the comparison between the theoretical methods and the data from ref 11 is more meaningful at temperatures in the interval between 200 and 400 K. Above $T = 400$ K the data from the literature are usually based on extrapolations from the experimental data obtained at lower temperatures and often make use of simple models (one-dimensional) to treat hindered rotations. The MUPEs are displayed in Figure 6. The calculated free energies by the GS2DT method yield MUPE-Gs larger than 20% at temperatures below $T = 700$ K. Those values are also larger than the obtained by the MS-T(C), so taking into account that the GS2DT method is computationally more demanding, the latter approximation is not pursued further. The values of C_p are not too sensitive to the method employed and the MS-T(U), MS-T(C) and E2DT methods yield similar errors in the whole interval of temperatures studied. At temperatures between 100 and 700 K the E2DT

method is substantially better than the rest, when compared with the "experimental" values of free energies, enthalpies and entropies. MS-T(C) is the second best method. This result indicates that accounting for torsional potential coupling is important in the evaluation of thermodynamic functions.

5 Conclusions

In this work we have presented a new benchmark torsional method, called E2DT, for systems with two coupled torsions, and we have used it to test several rovibrational partition functions (MS-HO, MS-T(U), MS-T(C) and GS2DT). For the tests we have used a set of 20 molecules with two hindered rotors for temperatures from 100 to 2500 K. From the results obtained and the comparison with experimental thermodynamic functions we draw the following conclusions:

i) The multi-structural reference classical rotational-torsional $Q^{\mathrm{MS-RCC(C)}}$ partition function when compared to the full coupled rotational-torsional partition function $Q^{\mathrm{FC(C)}}$ yields MUPEs that decrease from 15% to 8% at the lowest and highest temperatures studied, respectively.

ii) The accuracy of given rovibrational partition function depends not only on the accuracy of the anharmonic torsional partition functions but also on its implementation. Thus, globally separable torsional approximations, as the one used in the GS2DT method, do not improve the MS-T(C) results despite the fact that the former uses the 2D-NS method to calculate the torsional partition function.

iii) Although it leads to large errors above room temperature, the multi-structural harmonic approximation seems as good as any of the anharmonic methods described in this work when calculating rovibrational partition functions at room temperature or below. However, the comparison with the thermodynamic functions reported in the literature shows that approximations that include torsional anharmonicity and coupling perform also better than

the harmonic approximation at low temperatures.

iv) As noted previously,[10] the MS-T(U) method does not performs well if the two tops have very different barriers about each torsion.

v) Overall, the E2DT method chosen as benchmark for the comparison of the systems studied is also the method with the smallest MUPEs when compared with the available experimental thermodynamic functions.

vi) If the E2DT method is not affordable, the MS-T(C) method is the best option to calculate rovibrational partition functions including torsional anharmonicity. It only needs information about the conformational minima, which is a highly desirable characteristic when dealing with molecules having three or more hindered rotors.

Acknowledgement

The authors are grateful to Steven Mielke for comments on the manuscript. Financial support from Ministerio de Economia y Competitividad of Spain (Research Grant No CTQ2014-58617-R), the Consellería de Cultura, Educación e Ordenación Universitaria (Centro singular de investigación de Galicia acreditación 2016-2019, ED431G/09) and the European Regional Development Fund (ERDF), is gratefully acknowledged.

Supporting Information Available

For each of the 20 molecules it includes: a) ball and stick drawing of each conformation, b) reduced moments of inertia and product of the principal moments of inertia, c) ideal gas-phase standard-state thermodynamic functions (Gibbs free energy, enthalpy, entropy and heat capacity at constant pressure) at several temperatures, d) torsional angles and projected ZPE (ZPE excluding the torsional modes) for each stationary point, e) Cartesian coordinates, absolute energies and frequencies of each conformation, f) the parameters used to fit the kinetic and potential energy terms to Fourier series, g) torsional and rovibrational

partition functions described in this work at several temperatures.

References

(1) Zheng, J.; Yu, T.; Papajak, E.; Alecu, I. M.; Mielke, S. L.; Truhlar, D. G. Practical methods for including torsional anharmonicity in thermochemical calculations on complex molecules: The internal-coordinate multi-structural approximation. *Phys. Chem. Chem. Phys.* **2011**, *13*, 10885–10907.

(2) Meana-Pañeda, R.; Fernández-Ramos, A. Tunneling and conformational flexibility play critical roles in the isomerization mechanism of vitamin D. *J. Am. Chem. Soc.* **2012**, *134*, 346–354; (E) **2012**, *134*, 7193.

(3) Yu, T.; Zheng, J.; Truhlar, D. G. Multi-path variational transition state theory: rate constant of the 1,4-hydrogen shift isomerization of the 2-cyclohexylethyl radical. *J. Phys. Chem. A* **2012**, *116*, 297–308.

(4) Alecu, I. M.; Truhlar, D. G. Computational Study of the Reactions of Methanol with the Hydroperoxyl and Methyl Radicals. 2. Accurate Thermal Rate Constants. *J. Phys. Chem. A* **2011**, *115*, 14599–14611.

(5) Zheng, J.; Truhlar, D. G. Including torsional anharmonicity in canonical and microcanonical reaction path calculations. *J. Chem. Theory Comput.* **2013**, *9*, 2875.

(6) Zheng, J.; Yu, T.; Truhlar, D. G. Multi-structural thermodynamics of C-H bond dissociation in hexane and isohexane yielding seven isomeric hexyl radicals. *Phys. Chem. Chem. Phys.* **2011**, *13*, 19318–19324.

(7) Pitzer, K. S.; Gwinn, W. D. Energy levels and thermodynamic functions for molecules with internal rotations. I. Rigid frame with attached tops. *J. Chem. Phys.* **1942**, *10*, 428–440.

(8) Kilpatrick, J. E.; Pitzer, K. S. Energy levels and thermodynamics functions for molecules with internal rotation. III. Compound rotation. *J. Chem. Phys.* **1949**, *17*, 1064–1075.

(9) Zheng, J.; Mielke, S. L.; Clarkson, K. L.; Truhlar, D. G. *MSTor*: A program for calculating partition functions, free energies, enthalpies, entropies, and heat capacities of complex molecules including torsional anharmonicity. *Comput. Phys. Commun.* **2012**, *183*, 1803–1812.

(10) Zheng, J.; Truhlar, D. G. Quantum thermochemistry: multistructural method with torsional anharmonicity based on a coupled torsional potential. *J. Chem. Theory Comput.* **2013**, *9*, 1356–1367.

(11) Frenkel, M.; Marsh, K.; Wilhoit, R. C.; Kabo, G. J.; Roganov, G. N. In *Thermodynamics of organic compounds in the gas state*; Frenkel, M., Marsh, K., Eds.; Thermodynamics Research Center, College Station, TX, 1994.

(12) Fernández-Ramos, A. Accurate treatment of two-dimensional non-separable hindered internal rotors. *J. Chem. Phys.* **2013**, *138*, 134112.

(13) Simón-Carballido, L.; Fernández-Ramos, A. Calculation of the two-dimensional non-separable partition function for two molecular systems. *J. Mol. Model.* **2014**, *20*, 2190.

(14) Ellingson, B. A.; Lynch, V. A.; Mielke, S. L.; Truhlar, D. G. Statistical thermodynamics of bond torsional modes: Tests of separable, almost-separable, and improved Pitzer–Gwinn approximations. *J. Chem. Phys.* **2006**, *125*, 84305.

(15) Vansteenkiste, P.; Van Neck, D.; Van Speybroeck, V.; Waroquier, M. An extended hindered-rotor model with incorporation of Coriolis and vibrational-rotational coupling for calculating partition functions and derived quantities. *J. Chem. Phys.* **2006**, *124*, 044314; (E) **2006**, *125*, 049902.

(16) Fernández-Ramos, A.; Ellingson, B. A.; Meana-Pañeda, R.; Marques, J. M. C.; Truhlar, D. G. Symmetry numbers and chemical reaction rates. *Theor. Chem. Acc.* **2007**, *118*, 813–826.

(17) Pitzer, K. S. Energy levels and thermodynamic functions for molecules with internal rotations. II. Unsymmetrical tops attached to a rigid frame. *J. Chem. Phys.* **1946**, *14*, 239–243.

(18) Alves, T. V.; Simón-Carballido, L.; Ornellas, F. R.; Fernández-Ramos, A. Hindered rotor tunneling splittings: an application of the two-dimensional non-separable method to benzyl alcohol and two of its fluorine derivatives. *Phys. Chem. Chem. Phys.* **2016**, *18*, 8945–8953.

(19) Truhlar, D. G. A simple approximation for the vibrational partition-function of a hindered internal-rotation. *J. Comput. Chem.* **1991**, *12*, 266.

(20) Zhao, Y.; Lynch, B. J.; Truhlar, D. G. Hybrid meta Density Functional Theory methods for Thermochemistry, Thermochemical Kinetics, and noncovalent interactions: The MPW1B95 and MPWB1K models and comparative assessments for hydrogen bonding and van der Waals interactions. *J. Phys. Chem A* **2004**, *108*, 6908–6918.

(21) Hehre, W. J.; Ditchfield, R.; Pople, J. A. Self-consistent molecular orbital methods. XII. Further extensions of Gaussian-type basis sets for use in molecular orbital studies of organic molecules. *J. Chem. Phys.* **1972**, *56*, 2257–2261.

(22) Zhao, Y.; Schultz, N. E.; Truhlar, D. G. Design of density functionals by combining the method of constant satisfaction with parametrization for thermochemistry, thermochemical kinetics, and noncovalent interactions. *J. Chem. Theory Comput.* **2006**, *2*, 364–382.

(23) Alecu, I. M.; Zheng, J.; Zhao, Y.; Truhlar, D. G. Computational thermochemistry: Scale

factor databases and scale factors for vibrational frequencies obtained from electronic model chemistries. *J. Chem. Theory Comput.* **2010**, *6*, 2872–2887.

(24) *Gnuplot* 4.4: an interactive plotting program. http://gnuplot.sourceforge.net/, 2010.

(25) Renka, R. J. TRIPACK: a constrained two-dimensional Delaunay triangulation package. *ACM Transactions on Mathematical Software* **1996**, *22*, 1–8.

(26) Bollhöfer, M.; Notay, Y. *JADAMILU*: a software code for computing selected eigenvalues of large sparse symmetric matrices. *Comput. Phys. Commun.* **2007**, *177*, 951–964.

(27) Fernández-Ramos, A. *HR2D* version 2.0, Universidade de Santiago de Compostela, Santiago de Compostela. 2016.

(28) Zheng, J.; Meana-Pañeda, R.; Truhlar, D. G. *MSTor* version 2013: A new version of the computer code for the multi-structural torsional anharmonicity, now with a coupled torsional potential. *Comput. Phys. Commun.* **2013**, *184*, 2032–2033.

(29) Frisch, M. J.; Trucks, G. W.; Schlegel, H. B.; Scuseria, G. E.; Robb, M. A.; Cheeseman, J. R.; G.Scalmani,; Barone, V.; Mennucci, B.; Petersson, G. A.; Nakatsuji, H.; Caricato, M.; Li, X.; Hratchian, H. P.; Izmaylov, A. F.; Bloino, J.; Zheng, G.; Sonnenberg, J. L.; Hada, M.; Ehara, M.; Toyota, K.; Fukuda, R.; Hasegawa, J.; Ishida, M.; Nakajima, T.; Honda, Y.; Kitao, O.; Nakai, H.; Vreven, T.; Montgomery Jr., J. A.; Peralta, J. E.; Ogliaro, F.; Bearpark, M.; Heyd, J. J.; Brothers, E.; Kudin, K. N.; Staroverov, V. N.; Kobayashi, R.; Normand, J.; Raghavachari, K.; Rendell, A.; Burant, J. C.; Iyengar, S. S.; Tomasi, J.; Cossi, M.; Rega, N.; Millam, J. M.; Klene, M.; Knox, J. E.; Cross, J. B.; Bakken, V.; Adamo, C.; Jaramillo, J.; Gomperts, R.; Stratmann, R. E.; Yazyev, O.; Austin, A. J.; Cammi, R.; Pomelli, C.; Ochterski, J. W.; Martin, R. L.; Morokuma, K.; Zakrzewski, V. G.; Voth, G. A.; Salvador, P.; Dannenberg, J. J.; Dapprich, S.; Daniels, A. D.; Farkas, O.; Foresman, J. B.; Ortiz, J. V.; Cioslowski, J.; Fox, D. J. *Gaussian* 09, Gaussian, Inc., Wallingford CT, (2009).

(30) Meana-Pañeda, R.; Fernández-Ramos, A. Accounting for conformational flexibility and torsional anharmonicity in the H + CH_3CH_2OH hydrogen abstraction reactions: A multi-path variational transition state theory study. *J. Chem. Phys.* **2014**, *140*, 174303.

Table 1: Some parameters of interest for the conformers of the 20 systems studied, i.e., total number of wells, the symmetry numbers for internal rotation and the energy difference between conformers U_j (in cm^{-1}). It also indicates the two torsional angles ϕ_1, ϕ_2 of a given conformer, the MS-T(C) torsional frequencies $\overline{\omega}_{j,\eta}^{(C)}$, the normal-mode frequencies ω_j, and if that conformer has an enantiomer. For the other enantiomer $\phi_1 \rightarrow 360 - \phi_1$ and $\phi_2 \rightarrow 360 - \phi_2$.

System	*Wells*	σ_1, σ_2	*Conformer*	*Enantiomer?*	$[\phi_1, \phi_2]$	U_j	$\overline{\omega}_{j,\eta}$	ω_j
$S1$	4	1,1	S1-M1	No	180,0	0	153.4, 599.5	168.4, 668.0
			S1-M2	No	180,180	337	98.6, 589.8	100.4, 667.8
			S1-M3	No	0,180	787	92.4, 592.2	92.7, 677.3
			S1-M4	No	0,0	3334	78.5, 428.4	80.1, 430.5
$S2$	6	1,1	S2-M1	Yes	359,118	0	236.6, 181.1	248.8, 176.3
			S2-M2	Yes	199,109	535	268.6, 81.4	75.8, 260.9
			S2-M3	Yes	200,231	556	234.3, 69.4	64.9, 227.9
$S3$	4	1,1	S3-M1	No	0,0	0	201.6, 404.8	198.0, 392.6
			S3-M2	No	180,180	1189	86.7, 233.9	86.4, 227.9
			S3-M3	Yes	194,79	1295	81.9, 295.	81.4, 285.7
			S3-M4	No	0,180	2023	178.0, 259.5	165.6, 242.2
$S4$	9	1,3	S4-M1	No	180,60	0	294.9, 240.6	284.1, 241.3
			S4-M2	Yes	61,57	42	296.9, 265.0	284.2, 262.3
$S5$	5	1,1	S5-M1	No	0,0	0	118.3, 606.1	119.1, 641.6
			S5-M2	No	180,0	88	106.6, 565.0	112.7, 590.0
			S5-M3	No	0,180	2278	94.5, 473.5	94.2, 428.3
			S5-M4	Yes	158,171	2614	90.5, 479.4	94.5, 489.6
$S6$	4	1,1	S6-M1	No	0,0	0	209.4, 696.7	271.5, 900.2
			S6-M2	No	180,0	3641	147.5, 466.0	152.7, 542.5
			S6-M3	No	180,180	3695	148.1, 337.1	153.1, 264.4
			S6-M4	No	0,180	4789	137.7, 435.0	142.6, 475.7
$S7$	7	1,1	S7-M1	No	0,0	0	369.3, 104.2	373.4, 108.5
			S7-M2	Yes	199,142	50	433.1, 112.2	425.3, 118.2
			S7-M3	Yes	6,242	439	390.0, 88.4	398.9, 90.7
			S7-M4	Yes	156,354	1273	223.5, 105.8	217.0, 112.4
$S8$	9	1,3	S8-M1	No	0,60	0	241.9, 251.9	240.9, 261.3
			S8-M2	Yes	171,57	958	14.3, 157.2	28.2, 164.1
$S9$	9	1,1	S9-M1	Yes	6,60	0	180.2, 312.8	183.2, 302.6
			S9-M2	Yes	124,302	3	120.5, 350.1	118.8, 337.5
			S9-M3	No	0,180	202	161.5, 249.8	150.5, 244.9
			S9-M4	Yes	130,171	490	112.3, 257.0	111.1, 250.5
			S9-M5	Yes	123,65	576	107.4, 228.1	101.7, 222.9
$S10$	6	1,3	S10-M1	No	0,0	0	419.6, 180.8	423.8, 180.8
			S10-M2	No	180,0	781	232.8, 176.7	214.7, 169.3
$S11$	6	1,3	S11-M1	No	0,0	0	381.4, 52.7	329.2, 48.6
			S11-M2	No	180,0	209	210.4, 108.5	199.4, 99.1
$S12$	6	1,3	S12-M1	No	180,0	0	159.6, 139.2	179.1, 146.1
			S12-M2	No	0,0	1158	149.4, 106.9	111.9, 144.8
$S13$	5	1,1	S13-M1	No	180,0	0	107.2, 372.8	102.0, 290.8
			S13-M2	No	180,180	146	127.9, 257.0	131.4, 215.7
			S13-M3	Yes	39,6	233	134.2, 519.5	153.9, 595.8
			S13-M4	No	0,180	916	93.6, 301.3	107.5, 274.8
$S14$	7	1,1	S14-M1	No	180,0	0	135.7, 358.9	143.9, 370.0
			S14-M2	Yes	170,158	653	126.9, 279.6	141.0, 255.5
			S14-M3	Yes	30,2	1069	102.0, 405.6	102.1, 383.3
			S14-M4	Yes	41,198	1577	121.8, 306.0	123.7, 293.3
$S15$	9	1,3	S15-M1	No	180,0	0	122.0, 160.0	119.8, 158.0
			S15-M2	No	0,0	324	26.5, 146.0	13.6, 133.9
			S15-M3	No	0,60	325	40.4, 157.1	105.8, 196.2
$S16$	9	1,3	S16-M1	No	0,60	0	142.6, 304.6	166.5, 267.4
			S16-M2	Yes	239,61	25	109.4, 233.4	106.6, 228.5
$S17$	9	3,3	S17-M1	No	0,0	0	128.2, 130.5	120.8, 132.1
$S18$	6	1,1	S18-M1	No	180,180	0	108.2, 201.7	203.5, 278.7
			S18-M2	No	180,0	534	118.6, 192.6	126.6, 258.2
			S18-M3	Yes	27,179	1088	117.0, 174.3	125.2, 277.4
			S18-M4	Yes	30,0	1700	86.3, 190.9	80.9, 203.3
$S19$	6	2,1	S19-M1	Yes	36,59	0	53.3, 327.6	54.7, 320.9
			S19-M2	No	0,180	328	15.8, 228.0	8.0, 180.9
$S20$	6	1,3	S20-M1	No	180,60	0	349.1, 122.2	343.6, 90.6
			S20-M2	No	0,60	158	275.4, 163.1	289.4, 158.5

Table 2: Zero-point energies (in kcal/mol) of the global minimum of each system obtained by the harmonic oscillator (HO) and the E2DT approximations.

System	$\mathrm{ZPE}^{\mathrm{HO}}$	$\mathrm{ZPE}^{\mathrm{E2DT}}$
$S1$	27.37	27.24
$S2$	37.50	37.41
$S3$	38.21	38.26
$S4$	49.73	49.71
$S5$	42.11	42.09
$S6$	42.37	42.01
$S7$	48.40	48.37
$S8$	53.07	53.04
$S9$	52.96	52.91
$S10$	52.64	52.60
$S11$	52.79	52.80
$S12$	55.67	55.61
$S13$	56.27	56.29
$S14$	56.05	56.00
$S15$	55.85	55.84
$S16$	67.35	67.27
$S17$	66.96	66.95
$S18$	59.12	59.10
$S19$	83.00	82.99
$S20$	82.19	82.23

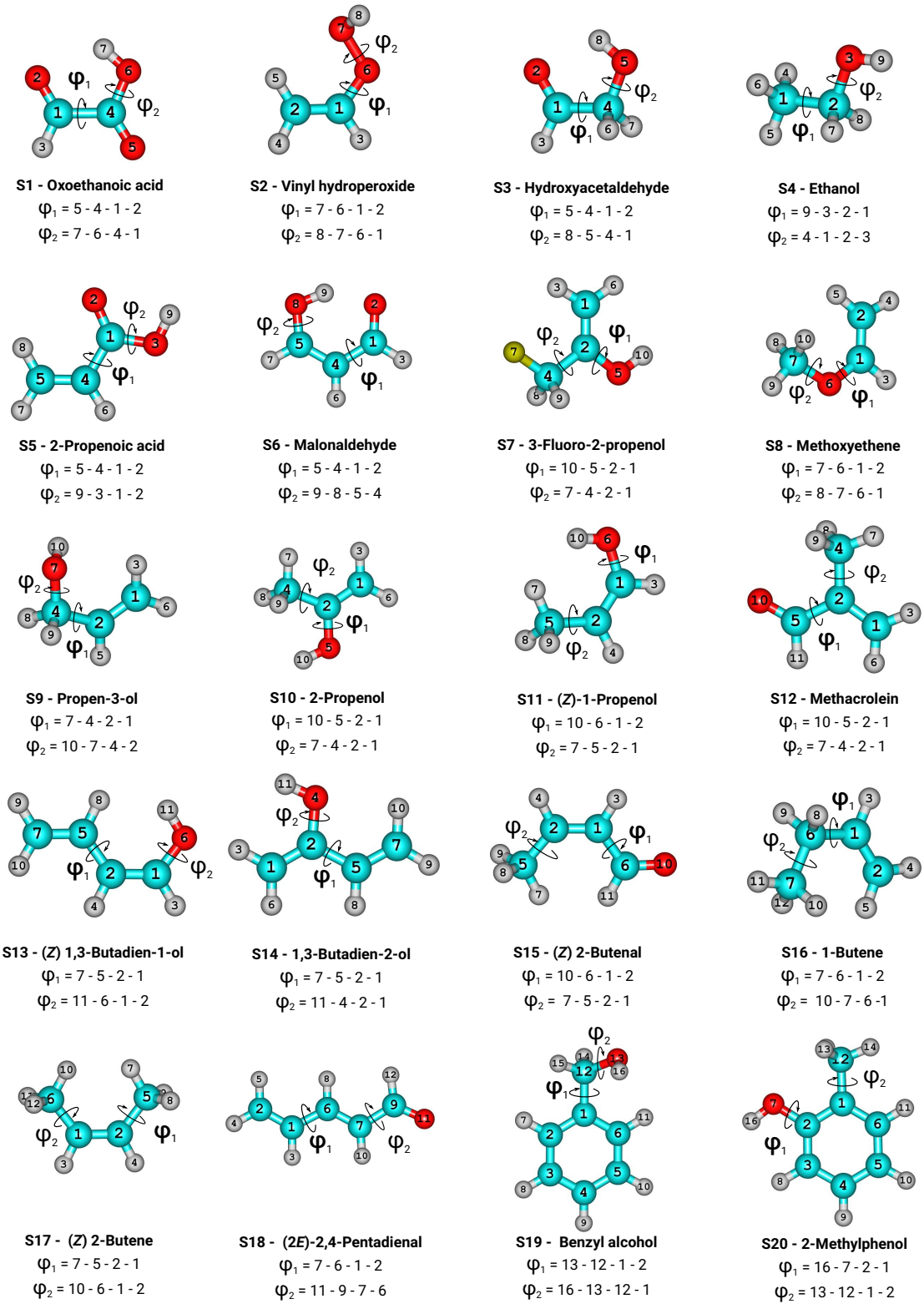

Figure 1: Molecules studied in this work. The two dihedral angles indicate the atoms involved in each torsional motion (C=cyan, O=red, H=gray, F=yellow).

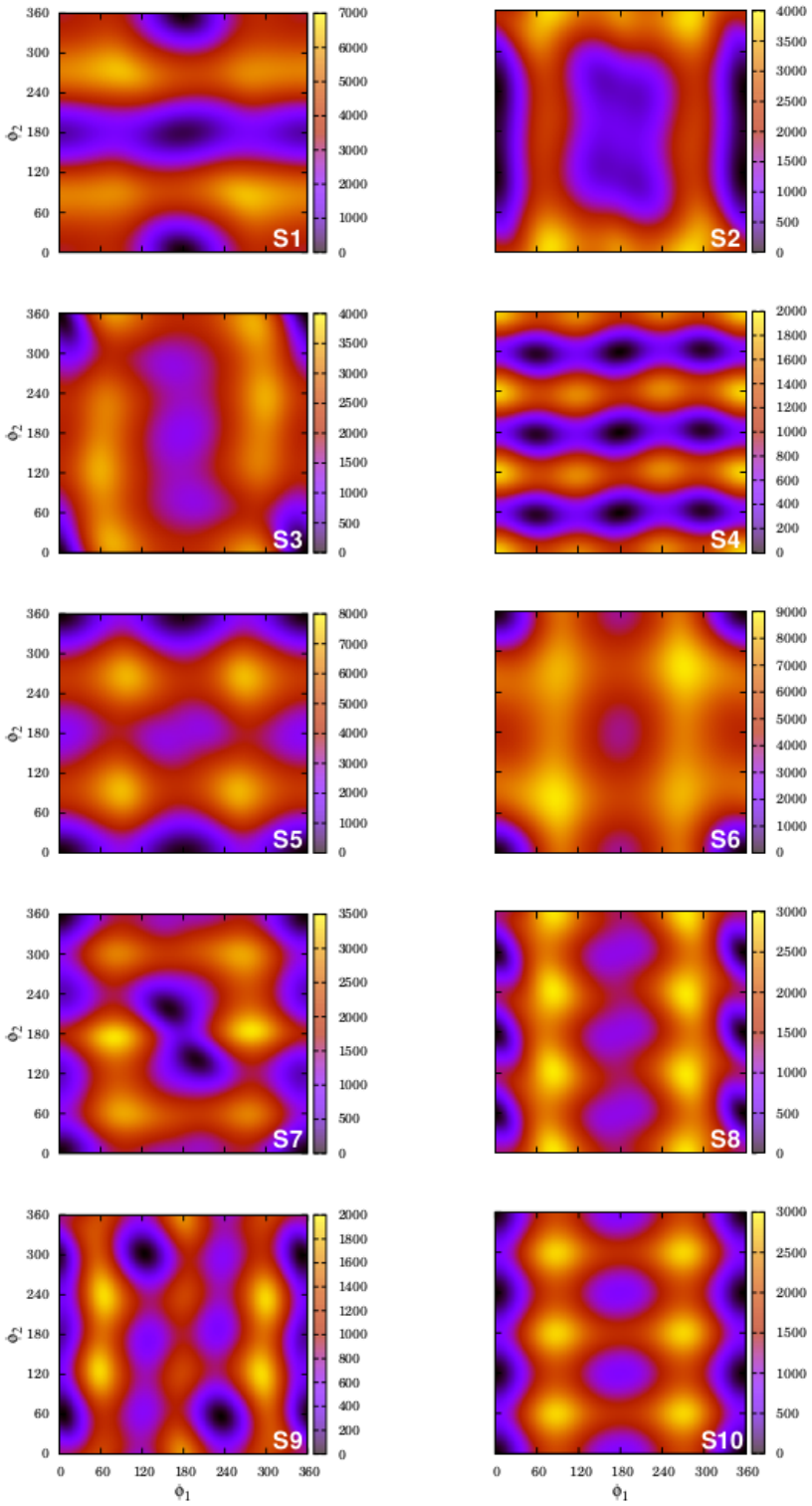

Figure 2: Contour plots for molecules **S1** to **S10**.

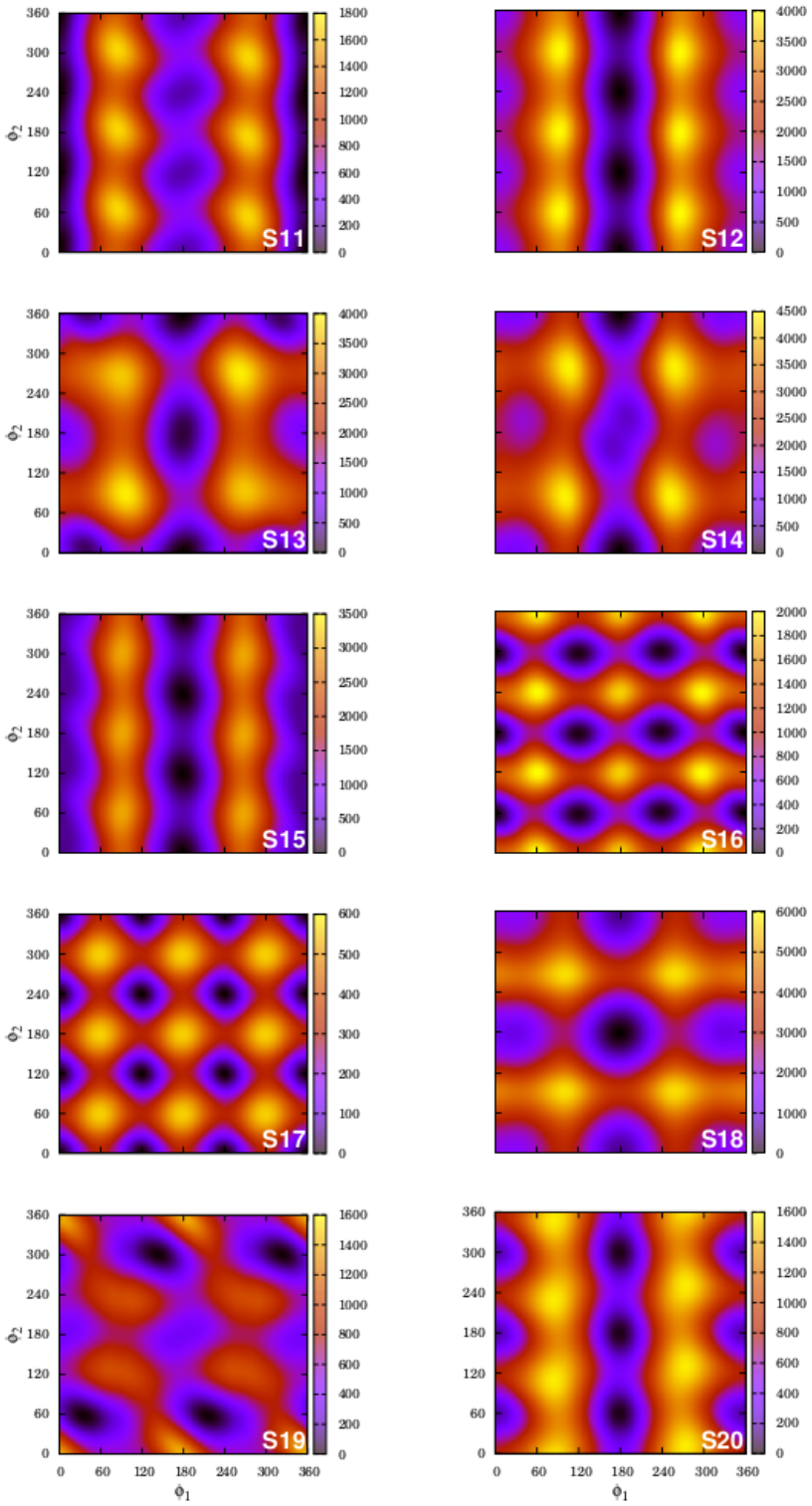

Figure 3: Same as 2 but for molecules **S11** to **S20**.

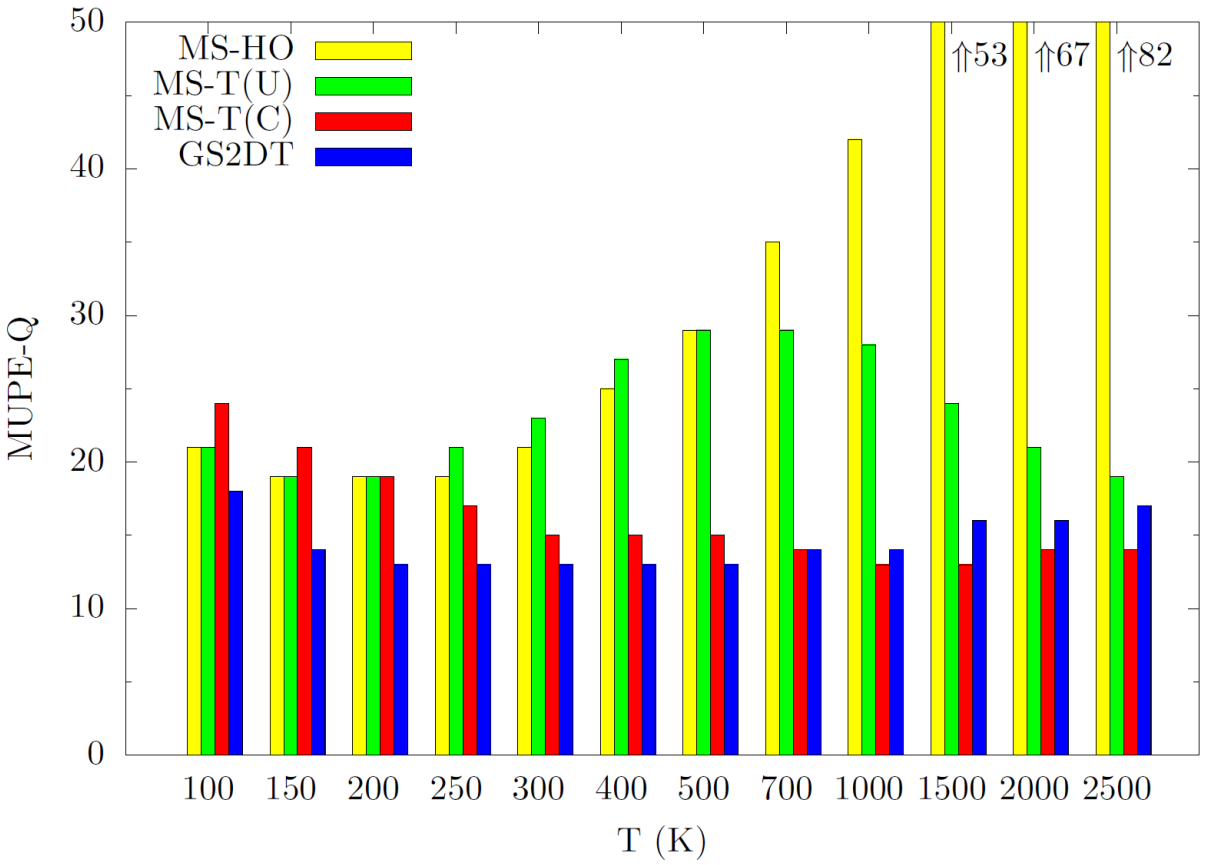

Figure 4: MUPE-Q calculated for several rovibrational partition functions at different temperatures (the E2DT method is the benchmark).

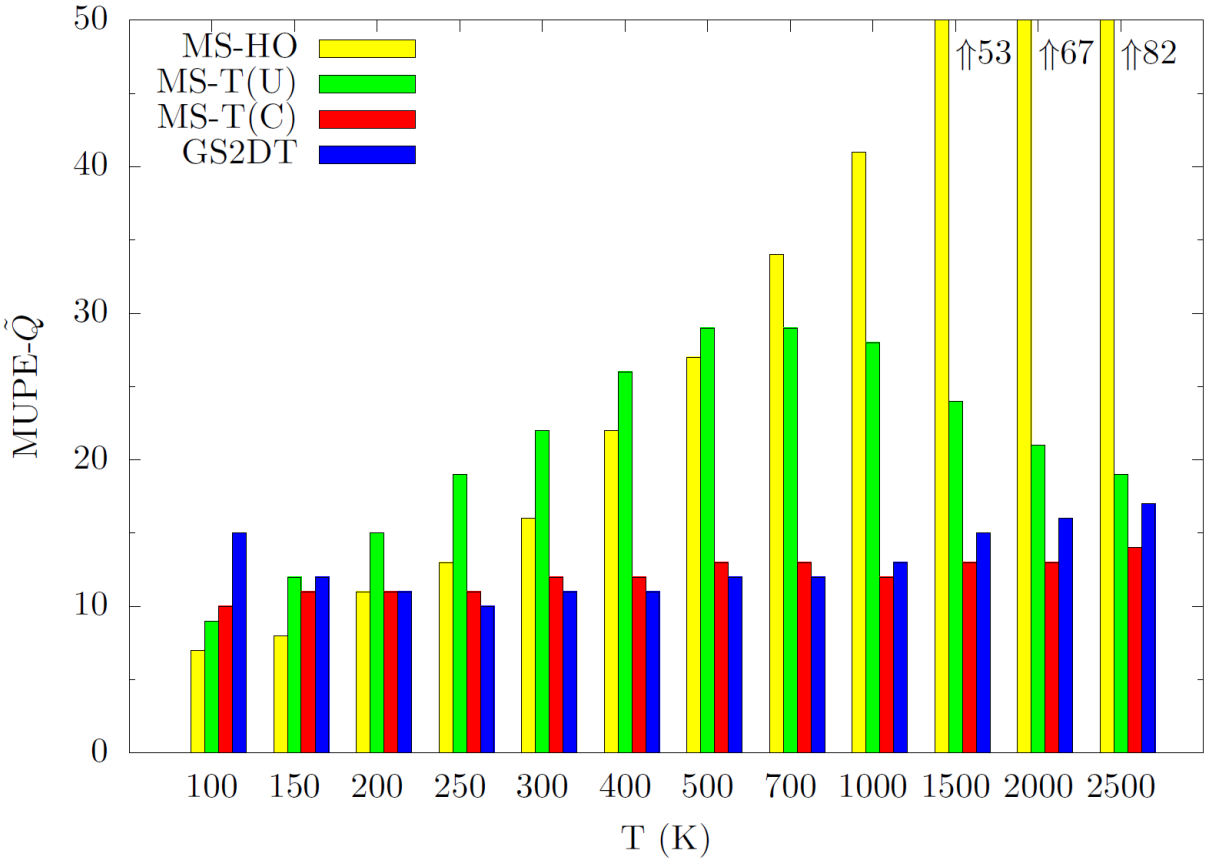

Figure 5: MUPE-$\tilde{Q}$ calculated for several torsional partition functions at different temperatures (the E2DT method is the benchmark).

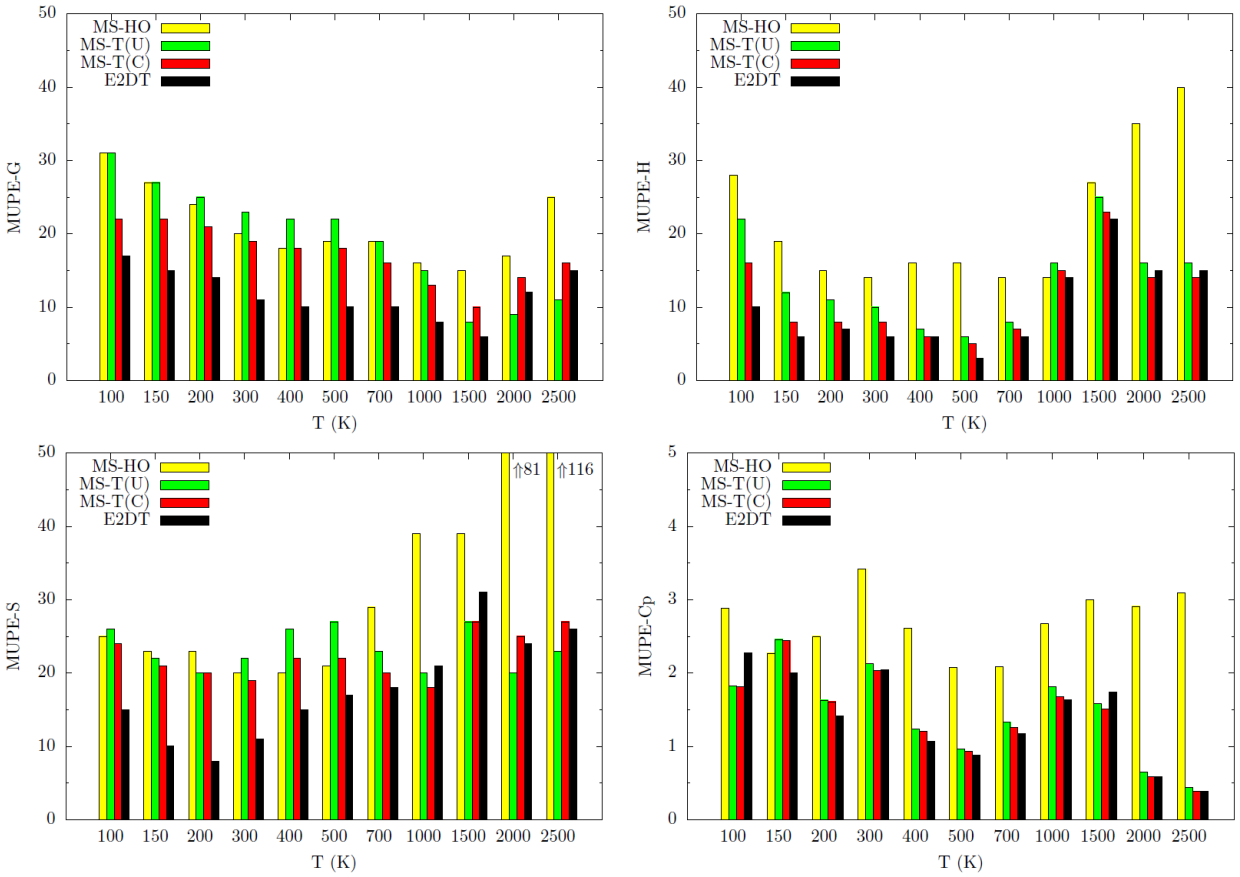

Figure 6: MUPEs obtained from the comparison for systems **S4**, **S16**, **S17**, **S5** and **S20** between gas-phase standard-state thermodynamic functions from the literature[11] (based at least in part on experimental data) and those obtained by various theoretical methods described in the main text.

For Table of Contents Only

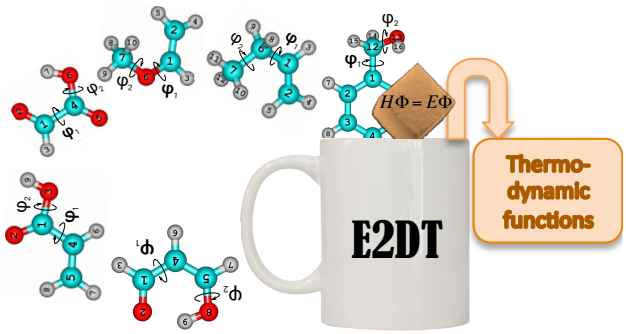

.